

## Full length article

## Detection of correlation characteristics between financial time series based on multi-resolution analysis

Xiang-Xin Wang<sup>a</sup>, Ling-Yu Xu<sup>a,b,\*</sup>, Jie Yu<sup>a,\*</sup>, Huai-Yu Xu<sup>c</sup>, Xuan Yu<sup>a</sup><sup>a</sup> School of Computer Engineering and Science, Shanghai University, NO. 333 Nanchen Road, Shanghai, China<sup>b</sup> Shanghai Institute for Advanced Communication and Data Science, Shanghai University, NO. 333 Nanchen Road, Shanghai, China<sup>c</sup> Shanghai Advanced Research Institute, Chinese Academy of Sciences, No. 99 Haik Road, Shanghai, China

## ARTICLE INFO

## Keywords:

Financial time series  
Wavelet decomposition  
Multi-resolution analysis  
Complex network

## ABSTRACT

Interactions between financial time series are complex and changeable in both time and frequency domains. To reveal the evolution characteristics of the time-varying relations between bivariate time series from a multi-resolution perspective, this study introduces an approach combining wavelet analysis and complex networks. In addition, to reduce the influence the phase lag between the time series has on the correlations, we propose dynamic time-warping (DTW) correlation coefficients to reflect the correlation degree between bivariate time series. Unlike previous studies that symbolized the time series only based on the correlation strength, the second-level symbol is set according to the correlation length during the coarse-graining process. This study presents a novel method to analyze bivariate time series and provides more information for investors and decision makers when investing in the stock market. We choose the closing prices of two stocks in China's market as the sample and explore the evolutionary behavior of correlation modes from different resolutions. Furthermore, we perform experiments to discover the critical correlation modes between the bull market and the bear market on the high-resolution scale, the clustering effect during the financial crisis on the middle-resolution scale, and the potential pseudo period on the low-resolution scale. The experimental results exactly match reality, which provides powerful evidence to prove that our method is effective in financial time series analysis.

## 1. Introduction

The stock market is a complex field that affords an enormous value to data mining. If we can predict the occurrence of a financial crisis or obtain the correlation characteristics between financial time series when a financial crisis occurs, then we can take relevant measures to minimize costs. Alternatively, if we can make predictions about the transaction price, closing price, turnover rate, etc., according to the historical trading data of certain stocks, then shareholders can make reasonable profit decisions. Hence, the analysis of financial time series is beneficial and essential to forecast economic conditions and prevent risks [1,2]. However, financial time series contain uncertainties. For example, there are various definitions of asset volatility, and for a stock return series, the volatility cannot be directly observed. As a result of the added uncertainty, it is impossible to detect the inner discipline of financial time series by simple observation; consequently, we should find appropriate methods to analyze financial time series.

Economic globalization and Internet communication have accelerated the integration of world financial markets in recent years.

Price movements in one market can spread easily and instantly to another market. For this reason, financial markets are more interdependent than ever before and must be considered together to better understand the dynamic structure of global finance. Therefore, in this paper, we focus on correlation analysis to explore the interaction patterns between bivariate financial time series. Moreover, the financial time series comprises different frequency components and such frequency components form a multiscale conformation behind the raw time series [3]. Scholars typically focused on the fluctuating correlation between the original time series, while the deeper potential information was ignored [4–7]. Therefore, we focus on multi-resolution analysis in this paper. Some studies have analyzed time series from multiple scales and have achieved valuable results in different research fields [3,8–10]. Gao and Li et al. [11] proposed a novel wavelet multiresolution complex network for analyzing multivariate nonlinear time series from the oil-water two-phase flow experiment. Gao and Zhang et al. [12] developed an adaptive optimal-Kernel time-frequency representation-based complex network method for characterizing fatigued behavior using the brain computer interface system. However, the correlation

\* Corresponding authors at: School of Computer Engineering and Science, Shanghai University, NO. 333 Nanchen Road, Shanghai, China (L.-Y. Xu, J. Yu).  
E-mail addresses: [xly@shu.edu.cn](mailto:xly@shu.edu.cn) (L.-Y. Xu), [jieyu@shu.edu.cn](mailto:jieyu@shu.edu.cn) (J. Yu).

characteristics of different scales have not been related to the special states in financial markets. Therefore, in this paper, we detect the correlation characteristics of special states in stock markets from different resolution scales.

In principle, the key idea behind correlation analysis in most studies is to calculate correlation coefficients [10] or the Granger causality [7]. However, these coefficients do not always remain unchanged over time. If we divide the original time series into different sub-series, then the evolution of the interaction behavior between bivariate time series can help reveal hidden dynamic interaction information. Furthermore, to reduce the influence of the phase lag between the time series on the correlation, we propose dynamic time-warping (DTW) correlation coefficients to reflect the correlation degree between bivariate time series. With regard to the multi-resolution analysis, wavelet decomposition offers an effective solution: representing the original time series as a function of two variables, namely, time and frequency [3]. Hence, the implementation of wavelet decomposition enables us to detect the evolution of different frequency components. In other words, a wavelet, working as a “microscope”, can observe the original time series using different “resolutions”. A finer resolution is better at detecting the details of an original signal, and a low resolution is well-suited for trend analysis [13].

In previous studies, mapping time series to complex networks has been widely applied to characterize nonlinear dynamic behaviors [14,15]. Gao et al. [16] presented a review of complex network analysis of time series. By analyzing the statistical characteristics of complex networks, such as influential nodes, betweenness centrality, and clustering, hidden information in time series can be captured [6,10,17]. In this paper, we raise a method combining wavelet analysis and complex network theory. To construct the networks, we first obtain the correlation patterns by a coarse-graining process. Being different from symbolizing the time series based only on correlation strength in the coarse-graining process [10], we set a second-level symbol based on the correlation length that could reflect the duration of a correlation strength. Then, we take the correlation patterns as nodes and the succeeding relations between patterns as edges. In the experimental part, we first verify the reliability and superiority of the wavelet decomposition applied to time series analysis through two comparative tests. After designing the multi-resolution evolutionary complex networks, we examine the statistical characteristics of these networks to provide investors with more information that cannot be captured by conventional analysis. To combine our method with practical applications, we analyze the correlation characteristics of special states in stock markets from three resolution scales. On the high-resolution scale, we verify the feasibility of regarding intermediary modes as the potential critical modes between the bull market and bear market by analyzing the betweenness centrality, which helps to predict the occurrence of a bull state or a bear state in the stock market. On the middle-resolution scale, the features of different financial crises have been detected by the cluster effect of the complex network, which can guide the shareholders to know the crisis features and make wise decisions. In addition, there is a potential pseudo cycle of the correlation relations between bivariate series in the stock market that is revealed by analyzing the dominant nodes and cluster effect on the low-resolution scale.

In summary, we make the following contributions:

- Considering the effects of the phase lag in the time series waveform, we propose DTW correlation coefficients to denote the correlation degree between bivariate time series.
- In the coarse-graining process, we first propose the correlation length to denote the duration of a certain correlation strength. The correlation length is beneficial to extract dynamic interaction information.
- A novel method combining wavelet decomposition and complex networks is designed to analyze the financial time series. And we first propose the idea of analyzing the special states in the stock

market from different resolutions. Experiments reveal that our method is effective in financial time series analysis.

The rest of the paper is structured as follows. Section 2 presents previous works of network construction. Section 3 introduces methods mapping time series to complex networks. Section 4 presents the experimental results and provides a discussion of the results, as well as the data used in our study. Finally, Section 5 concludes the paper.

## 2. Related works

With the in-depth research of complex networks, mapping time series to complex networks has become one of the mainstream approaches of time series analysis. Scholars focus on classification, prediction and correlation analysis of time series based on complex networks and have achieved many excellent results [18–25]. A complex network is a graph with special properties, which is the application of graph theory in practical engineering. Since Lacasa et al. proposed the well-known visibility graph algorithm to transfer time series into networks [26], the last decade has witnessed the effectiveness of complex networks in solving nonlinear problems in time series analysis of multiple domains [27–31], including turbulence [32], traffic networks [33], climate networks [34], brain networks [35] and multiphase flows [36], etc. Moreover, Zhang et al. [18] utilized link prediction based on visibility graph to preliminarily forecast the future and the accuracy was improved by fuzzy rules. With the accumulation of historical data, the scale of the network became increasingly larger, so Yang and Deng proposed a bio-inspired network division method to reduce the processing time [37].

There is ever-increasing body of methods for mapping nonlinear time series to complex networks that further address studies at the intersection of time series and complex network theory. The core idea of the visibility graph is to treat the time series as multiple numerical points, and then define the numerical point as a node of the network. Whether the nodes of a network are connected depends on whether the two numerical points can be seen and connected by each other in the displayed graph [26]. Xu and Zhang et al. proposed an improved visibility graph algorithm that maps time series to a weighted network rather than an unweighted network, and the weighted network greatly outperformed the unweighted network according to the performance comparison of the link prediction [23]. Zhang and Small proposed a mapping method that treats each periodic cycle as a basic node of a network [38]. If the phase space distance between the corresponding cycles is less than the predetermined value  $D$ , then the two nodes are considered to be connected. Marwan and Donges represented the adjacency matrix in complex network theory by the regression matrix calculated by the time series [39]. Connection between two nodes depends on whether the elements of the calculated adjacency matrix are zero. Additionally, some studies divided the original time series into pieces by fixed length windows or sliding windows, and then the connection relationship between nodes depends on the similarity or other characteristics of these segments [7,40].

However, the multiscale conformation problem in time series cannot be ignored because exploring time series from different resolutions is of great value for the analysis of nonlinear time series. It is widely acknowledged that the wavelet transform is a powerful tool for multi-resolution analysis. And wavelet analysis has begun to be incorporated into the analysis of time series and has achieved gratifying results in different research fields [41,42]. Gao and Li et al. [8] proposed a novel method combining wavelet entropy and complex networks for improving the electroencephalogram (EEG)-based fatigue driving classification and opened up new venues to address the challenge in EEG analysis. Research reported by Huang et al. [10] proposed an approach to explore the multiscale transmission characteristics of the correlation modes between bivariate time series. Huang and An et al. presented an algorithm for characterizing the evolution of

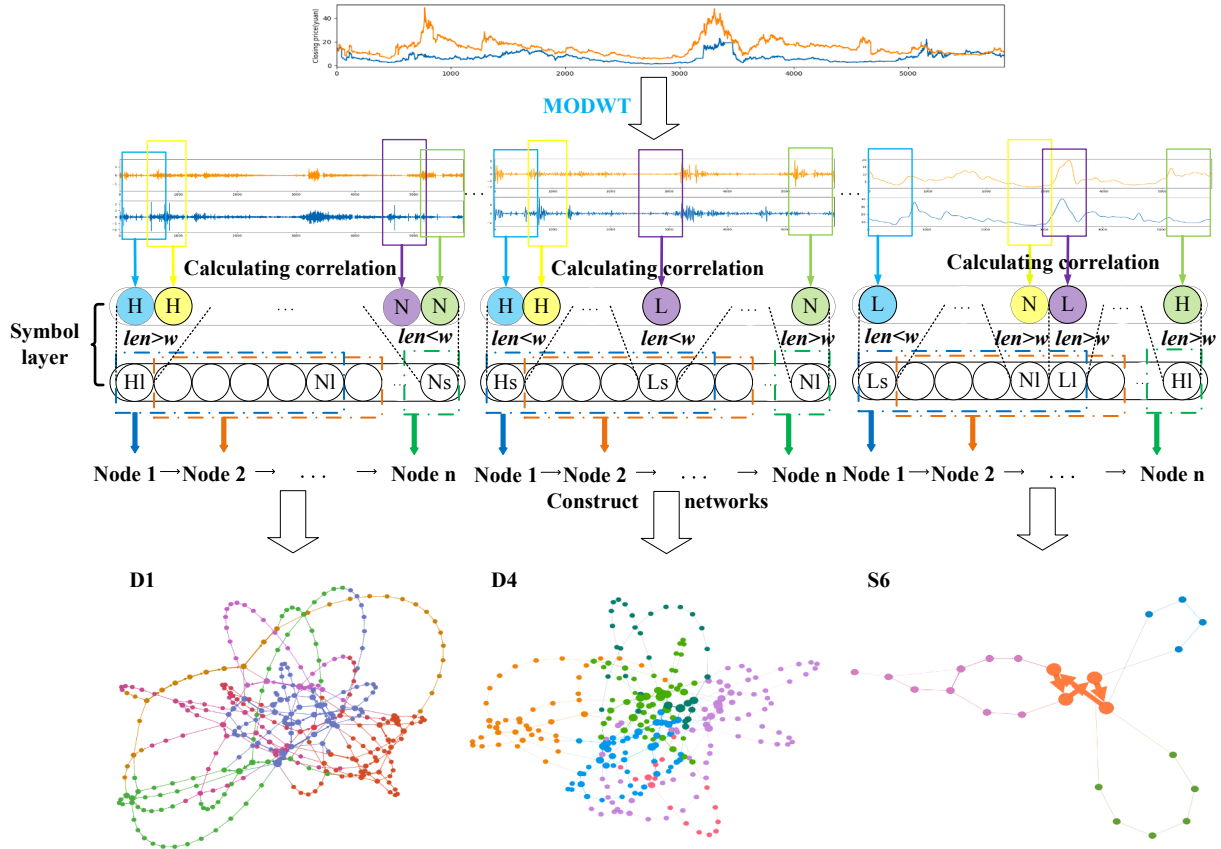


**Fig. 1.** The research framework based on the wavelet transform and complex networks. We choose scale D1, D4, and S6 as examples to show the process of constructing networks.

multiscale conformations with changes in time and frequency domains [43]. Although there are many methods for inferring complex networks from time series, these studies only focused on the correlation strength and lacked the correlation length, which uncovers the duration of a certain correlation strength and is beneficial to extract dynamic interaction information. Furthermore, the influences between stocks are not in real time, and thus, there is a time lag, which is the phase lag reflected in the time series waveform. Almost all of these studies calculated correlation coefficients based on the Pearson correlation, without considering the effects of the phase lag. Considering the above, we propose a novel mapping method combining two-level symbolization and DTW correlation coefficients. Our approach perfectly solves these problems, so it is more capable of reflecting the evolution of the relationship between financial time series. Moreover, we first propose the idea of analyzing the special states in the stock market from different resolutions, which is the most important contribution of our work.

### 3. Mapping time series to complex networks

In this section, we introduce a new method to construct complex networks. First, we employ the maximal overlap discrete wavelet transform (MODWT) to decompose the raw series into time-frequency domains. Next, we construct the multi-resolution evolutionary complex networks based on the obtained wavelet series.

#### 3.1. Decomposition in joint time-frequency domains

To reveal the relationship between the time series from different resolutions, we first use the wavelet transform to decompose the raw sequence into the time-frequency domains. More specifically, the traditional method of time series analysis merely used one single value to

describe the correlation extent between two time series, whereas we can obtain accurate correlation coefficients of different frequency scales by wavelet decomposition and correlation calculation methods. In addition, the MODWT, which is far more desirable in financial applications, was chosen to decompose the time series [44–46]. The process of MODWT is similar to the definition of discrete wavelet transform (DWT) [47]: suppose that the wavelet filter  $\{\tilde{h}_{j,l}\} = h_{j,l}/2^{j/2}$  and scaling filter  $\{\tilde{g}_{j,l}\} = g_{j,l}/2^{j/2}$  are defined for this decomposition, and the  $l = 1, \dots, L$  represents the length of the filters while  $j$  indicates the level of decomposition. For the time series  $\{X_t : t = 0, \dots, N - 1; N = 2^n, n \in \mathbb{Z}\}$ , the  $j$ th level MODWT wavelet ( $\tilde{W}_j$ ) and scaling ( $\tilde{V}_j$ ) coefficients are described as:

$$\tilde{W}_j = \tilde{\omega}_j X_t \quad \text{and} \quad \tilde{V}_j = \tilde{v}_j X_t$$

where each row of the  $N \times N$  matrix  $\tilde{\omega}_j$  contains values denoted by  $\{\tilde{h}_{j,l}\}$ , whereas  $\tilde{v}_j$  contains values denoted by  $\{\tilde{g}_{j,l}\}$ .  $\tilde{\omega}_j$  can be written as:

$$\tilde{\omega}_j = \frac{1}{2^k} \begin{bmatrix} \tilde{h}_{j,0} & \tilde{h}_{j,0} & \tilde{h}_{j,0} & \tilde{h}_{j,0} & \tilde{h}_{j,0} & \tilde{h}_{j,0} & \tilde{h}_{j,0} \\ \tilde{h}_{j,1} & \tilde{h}_{j,1} & \tilde{h}_{j,1} & \tilde{h}_{j,1} & \tilde{h}_{j,1} & \tilde{h}_{j,1} & \tilde{h}_{j,1} \\ \tilde{h}_{j,2} & \tilde{h}_{j,2} & \tilde{h}_{j,2} & \tilde{h}_{j,2} & \cdots & \tilde{h}_{j,2} & \tilde{h}_{j,2} \\ \vdots & \vdots & \vdots & \vdots & \cdots & \vdots & \vdots \\ \tilde{h}_{j,N-2} & \tilde{h}_{j,N-2} & \tilde{h}_{j,N-2} & \tilde{h}_{j,N-2} & \tilde{h}_{j,N-2} & \tilde{h}_{j,N-2} & \tilde{h}_{j,N-2} \\ \tilde{h}_{j,N-1} & \tilde{h}_{j,N-1} & \tilde{h}_{j,N-1} & \tilde{h}_{j,N-1} & \tilde{h}_{j,N-1} & \tilde{h}_{j,N-1} & \tilde{h}_{j,N-1} \end{bmatrix} \quad (1)$$

while  $\tilde{v}_j$  is expressed as above with each  $\{\tilde{h}_{j,l}\}$  replaced by  $\{\tilde{g}_{j,l}\}$ . Therefore, after the MODWT of level  $J$ , we can obtain several wavelet series  $D_1, D_2, \dots, D_J$  and  $S_j$  with the same length of raw series. The decomposition process is shown as follows:

$$X_t = \sum_{j=1}^J \tilde{\omega}_j^T \tilde{W}_j + \tilde{v}_j^T \tilde{V}_j = \sum_{j=1}^J \tilde{D}_j + S_j \quad (2)$$

where  $j$  is the decomposition level,  $D_j$  and  $S_j$  are the wavelet details and approximation respectively.

### 3.2. Constructing the multi-resolution evolutionary complex networks

After decomposing the bivariate time series, we obtain the output of the MODWT, including  $J$  levels of wavelet details and one smooth trend at the maximum level, being expressed as wavelet series  $D_{x,j}$ ,  $D_{y,j}$ ,  $S_{x,J}$  and  $S_{y,J}$ . Next, we construct multi-resolution evolutionary complex networks according to the following three key steps:

- (1) calculate correlation coefficients and divide the correlation strength,
- (2) obtain correlation patterns by coarse-graining processing, and
- (3) construct the multi-resolution evolutionary complex networks.

The whole process of constructing complex networks is shown in Fig. 1. As the level of decomposition increases, the wavelet series tend to be smoother, and the wavelet approximation  $S_j$  is the smoothest. Therefore, in order to show the differences in complex networks due to the different decomposition levels, we select scale D1, D4, and S6 as examples to show the process of constructing networks. After turning the raw series into wavelet series by MODWT, we divide the correlation strength ( $H, L, N$ ) into the first-level label according to the correlation coefficients of sub-series. If the correlation length is larger than threshold  $w$ , we set the second-level label as  $l$ , and  $s$  in contrast, which will be described in detail below. Obtaining correlation patterns by the coarse-graining process, we take the correlation patterns as nodes and the succeeding sequence relations between patterns as edges to form the complex networks. In a complex network, nodes of the same color belong to the same cluster. Moreover, the higher the decomposition level is, the smaller the resolution tends to be, and as a result, the nodes in networks become larger and fewer.

*Calculate correlation coefficients and divide the correlation strength:* Dynamic time-warping proposed by Sakoe [48] is always used to align two time sequences of potentially different lengths and measure the similarity between them. Moreover, DTW finds the correspondence between points from the two sequences by warping them in the time domain [49]. The essence of warping is to overcome the influence of the phase lag between series. The influences between stocks are not in real time and there is a time lag, which is the phase lag reflected in the time series waveform. Therefore, DTW is used although the bivariate time series in this paper are of the same length. Given two series  $X_t = \{x_1, x_2, \dots, x_m\}$  and  $Y_t = \{y_1, y_2, \dots, y_n\}$ , the DTW distance is defined as follows:

$$\text{dtw}(X_t, Y_t) = \min\left(\frac{1}{k} \sum_{\alpha=1}^k w_\alpha\right) \quad (3)$$

where  $w_\alpha$  indicates that the  $i$ th point in sequence  $X_t$  matches the  $j$ th point in sequence  $Y_t$ , and  $k$  denotes the length of the warping path. Before calculating the correlation coefficients, we use the sliding window to divide the raw series into pieces. The window can be set with different scales according to different analysis needs. If we desire to understand the transition characteristics in the short term, the length of the window should be set to a smaller value. In contrast, a larger window size should be adopted when the goal is to obtain a better understanding of the transmission characteristics for long periods. As the length of the sliding window increases, the number of nodes and edges in the corresponding complex networks decreases (Fig. 2). When the window size is 60, the number of nodes is only 49. An increase in the length of the window will hide the characteristics of the diversity of the correlation patterns. Thus, if the value of the window size is too

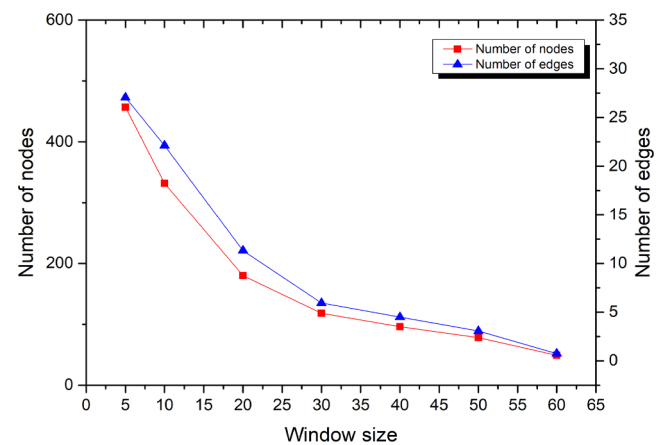


Fig. 2. Variation of the number of the nodes and edges in networks with different window sizes.

large, it is meaningless for studying the transmission of the correlation patterns in financial time series. Because we want to demonstrate the multi-resolution phenomenon in the transmission process of correlation patterns, we should select a relatively small size for the sliding window: 10 days.

After dividing the wavelet series, we obtain an array of sub-series. For example, the wavelet series  $D_{x,1}$  and  $D_{y,1}$  both obtain  $(N - 9)$  sub-series at the  $1$ th decomposition level, where  $N$  denotes the length of series. Then, we compute the DTW distance of each pair corresponding sub-series and obtain a matrix of DTW distances:

$$D_{X,Y} = \begin{bmatrix} \text{dtw}(D_{x,1,1}, D_{y,1,1}) \text{dtw}(D_{x,1,2}, D_{y,1,2}) \cdots \text{dtw}(D_{x,1,N-9}, D_{y,1,N-9}) \\ \text{dtw}(D_{x,2,1}, D_{y,2,1}) \text{dtw}(D_{x,2,2}, D_{y,2,2}) \cdots \text{dtw}(D_{x,2,N-9}, D_{y,2,N-9}) \\ \vdots & \vdots & \vdots \\ \text{dtw}(D_{x,J,1}, D_{y,J,1}) \text{dtw}(D_{x,J,2}, D_{y,J,2}) \cdots \text{dtw}(D_{x,J,N-9}, D_{y,J,N-9}) \end{bmatrix} \quad (4)$$

where  $D_{y,J,N-9}$  denotes the  $(N - 9)$ th sub-series of the  $J$ -level wavelet series. To transform DTW distance to the correlation coefficient, we should enact some processes. According to the definition of DTW distance, the smaller the distance is, the more similar two series are. First, we acquire the reciprocal of the elements in matrix  $D_{X,Y}$ . Next, we normalize the values of each row. Therefore, the values of the matrix  $D_{X,Y}$  are limited to 0–1 and we obtain a new correlation coefficient matrix  $S_{X,Y}$ :

$$S_{X,Y} = \begin{bmatrix} ds(D_{x,1,1}, D_{y,1,1}) ds(D_{x,1,2}, D_{y,1,2}) ds(D_{x,1,N-9}, D_{y,1,N-9}) \\ ds(D_{x,2,1}, D_{y,2,1}) ds(D_{x,2,2}, D_{y,2,2}) ds(D_{x,2,N-9}, D_{y,2,N-9}) \\ \vdots & \vdots & \vdots \\ ds(D_{x,J,1}, D_{y,J,1}) ds(D_{x,J,2}, D_{y,J,2}) ds(D_{x,J,N-9}, D_{y,J,N-9}) \end{bmatrix} \quad (5)$$

where  $ds$  denotes the value of the DTW distance after the processes of finding the reciprocal of matrix elements and normalization. Therefore,  $ds$  are capable of representing DTW correlation coefficients of two sub-series. To make the correlation degree more specific, we define three correlation levels which are symbolized as follows:

$$cs = \begin{cases} H, ds(D_{x,i,j}, D_{y,i,j}) \in [0.7, 1] \\ L, ds(D_{x,i,j}, D_{y,i,j}) \in [0.3, 0.7] \\ N, ds(D_{x,i,j}, D_{y,i,j}) \in [0, 0.3] \end{cases} \quad (6)$$

*Obtain correlation patterns by coarse-graining processing:* Coarse-graining is useful in identifying the correlation patterns, because it preserves the trajectory of the fluctuations. First, after determining the rank of correlation coefficients, we obtain the first-level label. In addition, we choose the closing prices of PingAn Bank (PAB) stock and Beijing Grains Holding (BGH) stock in China's market from 29 March 1994 to 29 March 2018 as samples. The symbolic process of the

**Table 1**

The process of setting the first-level label for the correlation between the 1st wavelet series of the PAB and BGH.

No.	PAB-1	BGH-1	Correlation coefficient	Correlation symbol
1	1.19812	1.56156		
2	-0.0534	-0.1653		
3	-0.2656	-0.1657		
4	0.05156	-0.0359		
5	-0.0218	-0.0093		
6	-0.0515	-0.0531		
7	0.01093	0.03593		
8	0.03593	0.10246		
9	-0.0640	-0.1078		
10	-0.0437	-0.0257	0.97375	H
11	0.16875	0.04843	0.86102	H
12	-0.3187	0.10468	0.80942	H
13	0.23593	-0.2703	0.82687	H
14	0.06875	0.21875	0.82322	H
15	-0.1359	0.09375	0.76888	H
16	-0.0828	-0.1078	0.62460	L
17	0.20156	-0.2140	0.56048	L
18	-0.0906	0.28125	0.56414	L
19	-0.0078	-0.0857	0.58232	L
20	0.01375	-0.0625	0.56573	L
...	...		...	...
5839	-1.1696	-1.5809	0.25846	N

Sliding window 1

correlation between the 1st level wavelet series of PingAn Bank (PAB-1) and Beijing Grains Holding (BGH-1) is given by [Table 1](#).

However, to explore the dynamic evolutionary relationship between time series, it is not sufficient to consider only the correlation strength because the duration of a specific correlation strength is obscure. Hence, in this paper, based on the work of the first-level label, we set the second-level label to embody the correlation length of bivariate time series, i.e., the persistence extent of a specific correlation strength. According to the label series obtained by the first-level label, we set the duration length of a specific correlation strength as  $len$ . Letting the label series  $\{H, H, L, H, N, L, L, L\}$  serve as an example, we can acquire  $len_{H,1} = 2$ ,  $len_{L,1} = 1$ ,  $len_{H,2} = 1$ ,  $len_{N,1} = 1$ ,  $len_{L,2} = 3$ , where the subscript letters represent correlation strength labels, and the subscript numbers represent the order in which they appear. For the threshold  $\omega$ , we set the second-level label to 1 on the condition of  $len > \omega$ , while we set the second-level label to 0 if  $len \leq \omega$ . The symbolization process is as follows:

$$cd = \begin{cases} Hl(ds(D_{x,i,j}, D_{y,i,j})) \in [0.8, 1] \text{ and } len_H > \omega \\ Hs(ds(D_{x,i,j}, D_{y,i,j})) \in [0.8, 1] \text{ and } len_H < \omega \\ Ll(ds(D_{x,i,j}, D_{y,i,j})) \in [0.3, 0.8) \text{ and } len_L > \omega \\ Ls(ds(D_{x,i,j}, D_{y,i,j})) \in [0.3, 0.8) \text{ and } len_L < \omega \\ Nl(ds(D_{x,i,j}, D_{y,i,j})) \in [0, 0.3) \text{ and } len_N > \omega \\ Ns(ds(D_{x,i,j}, D_{y,i,j})) \in [0, 0.3) \text{ and } len_N < \omega \end{cases} \quad (7)$$

To ascertain that there are six symbols representing the different correlation features in one correlation pattern at least once, we choose six symbols in successive order as a correlation pattern. Additionally, we use the second-level sliding window to unveil the transmission process from one correlation mode to another, and the sliding window slides at a 1-symbol interval. Hence, the process of setting the second-level label and the procedure of coarse-graining are given in [Table 2](#). The transmission process reflects that the correlation features change over time.

**Construct the multi-resolution evolutionary complex networks:** Based on the above progress, we can obtain the coarse-graining modes as the correlation patterns in the evolution process under each observation resolution. Because the conversion between two types of correlation

patterns would repeat in the transition process, the trajectory of the conversion among correlation patterns forms a network. To map the evolutionary network, we take the correlation patterns as nodes and the connections between the successive patterns as edges. The weight of an edge is the frequency of the transition between two types of correlation patterns. Next, the networks can be constructed at each scale to reveal how the correlation patterns of bivariate time series transfer with each other in different time-frequency domains.

#### 4. Experimental analysis and discussion

##### 4.1. Materials

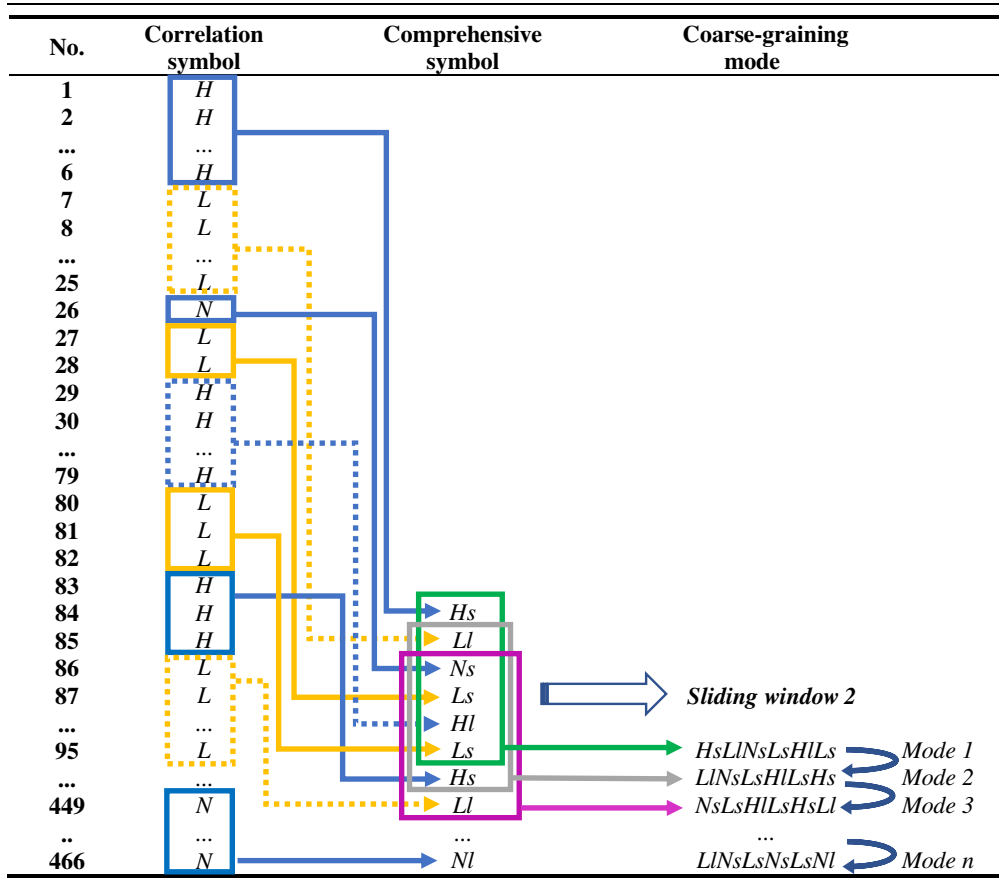
In China's stock market, bank shares account for approximately 15% of the A-share market, which ranking first in proportion. Fluctuations in bank shares are more likely to have an impact on the fluctuations of other shares. Therefore, aiming to analyze the dynamic correlation features of bivariate time series, we select PingAn Bank (PAB) stock in A-share as one sample. In addition, Beijing Grains Holding (BGH) stock is randomly chosen to guarantee the generality of the analysis results. The data are the closing price of two stocks from 29 March 1994 to 29 March 2018, which contain 5839 daily observations.

##### 4.2. Wavelet decomposition

In this part, we will discuss three aspects of the process of wavelet decomposition: (1) determination of decomposition level, (2) rationale of wavelet decomposition, (3) results of wavelet decomposition.

**Determination of decomposition level:** In this paper, the optimal level of multiscale decomposition is determined according to the minimization of the Shannon entropy criterion. It is estimated on the basis of the selected wavelet class, the sample length and the boundary-distortion method. The entropy of each level is estimated step-wise, and it is compared with the one from the previous level. If it decreases, then the new decomposition "reveals" interesting, non-redundant information and the decomposition continues. The optimal level is determined at the minimum-value of the entropy-related criterion. Let  $\tilde{D}_{y,j}$  represent the details and the  $j$ th level approximation coefficient of  $Y_t$  for scales

**Table 2**  
The process of setting the second-level label and obtaining correlation patterns.



$j = 1, \dots, J$  in an orthonormal basis [50,51]. The Shannon entropy for the coefficients in each level is defined as:

$$E_{\text{Shannon}}(\tilde{D}_{y,j}) = -\tilde{D}_{y,j}^2 \cdot \log(\tilde{D}_{y,j}^2) \quad (8)$$

and thus, for the entire time series, it is  $E_{\text{Shannon}}(Y_t) = -\sum_j \tilde{D}_{y,j}^2 \cdot \log(\tilde{D}_{y,j}^2)$  with the convention  $0 \cdot \log(0) = 0$ . Table 3 indicates the optimal minimum-entropy estimation for the PingAn Bank stock and Beijing Grains Holding stock closing price series. Both the optimal decomposition level of PAB and BGH are six according to the minimum value of the Shannon entropy criterion. Hence, the closing price series are decomposed into D1–D6 details and the 6th-level smooth approximation, and those coefficients can be used to reconstruct the original time series.

*Rationale of wavelet decomposition:* To demonstrate the reliability and superiority of the wavelet decomposition applied to time series analysis, we establish two sets of performance comparison experiments.

Firstly, the analysis of financial time series is primarily based on an important assumption that the sequence is stationary. After decomposition by MODWT, the sequence become smoother. We compare it with the traditional time series decomposition method (seasonal-trend decomposition [52]). The stationarities of the sub-series obtained by the two methods are analyzed, and the results of the stationarity tests of

**Table 4**  
Results of stationarity tests.

Method	Augmented Dickey-Fuller test			
	T-Statistic	Critical Value	p-Value	Confidence Level
Seasonal-Trend Decomposition	residual	-20.493	-3.43	0.0001 1%
	seasonal	-14.207	-3.43	0.0002 1%
	trend	-2.898	-3.43	0.046 1%
			-2.86	5%
MODWT	1-modwt	-33.058	-3.43	0.0001 1%
	2-modwt	-28.223	-3.43	0.0001 1%
	3-modwt	-21.192	-3.43	0.0001 1%
	4-modwt	-14.445	-3.43	0.0002 1%
	5-modwt	-10.669	-3.43	0.0002 1%
	6-modwt	-7.100	-3.43	0.0002 1%
	s-modwt	-4.503	-3.43	0.0003 1%

*Note:* We choose ADF (Augmented Dickey-Fuller test) as the stationarity test method and T-Statistic as the statistic. Different confidence levels correspond to different critical values, e.g., 1% corresponds to -3.43, 5% corresponds to -2.86. If the T-Statistic value is smaller than the critical value and the p-value is smaller than the confidence level, we can reject the null hypothesis for the associated statistical tests at the confidence level.

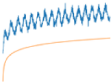
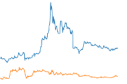
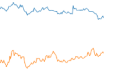
**Table 3**  
Shannon entropy of the multi-level wavelet series and the raw series.

Wavelet scale	Raw	1	2	3	4	5	6	7	8
PAB-Ent	1.176	0.562	0.524	0.502	0.495	0.463	0.457	0.763	1.352
BGH-Ent	1.228	0.636	0.621	0.611	0.607	0.613	0.503	0.812	1.261

sub-series are shown in Table 4.

From Table 4, the seasonal-trend decomposition method can break the sequence into three parts: *trend*, *seasonal*, and *residual*. The *residual* and *seasonal* can be regarded as stationary series when the confidence level is 1%. However, the *trend* is viewed as a non-stationary series because the value of the T-Statistic is larger than the critical value, and

**Table 5**  
Comparison test of different methods of calculating the correlation degree.

				
Pearson	0.7667	0.1468	0.0652	0.6171
Kendall	0.6654	0.1326	0.0579	0.2428
1-modwt	0.2810	0.3603	0.0203	0.8036
2-modwt	0.5137	0.2999	-0.0497	0.7270
3-modwt	0.6754	0.0947	0.2156	0.6619
4-modwt	0.8190	0.3282	0.0940	0.5875
5-modwt	0.8771	0.2011	0.3438	0.8110
6-modwt	0.8946	0.2039	-0.7986	0.5762
s-modwt	0.9417	0.1477	-0.8434	0.5994

the p-value is not smaller than the confidence level. Compared with the seasonal-trend decomposition method, all the sequences obtained using the MODWT can be regarded as stationary sequences when the confidence level is 1%. At the same confidence level, the smaller the T-Statistic value is, the more stable the sequence is. Therefore, the wavelet method is superior to the traditional decomposition method in terms of stationarity.

Secondly, multi-resolution analysis gives us the opportunity to observe data from multiple perspectives. Wavelet decomposition is a typical method of multi-resolution analysis. We devise another comparative experiment in order to prove the superiority of multiscale analysis in time series analysis. There are many methods to measure the correlation between bivariate time series, e.g., Pearson and Kendall correlations. We select three segments from the original bivariate financial series randomly, and a set of bivariate series composed of the logarithmic function and the superposition of the logarithmic and sine functions. First, the Pearson and Kendall coefficients of these bivariate time series are calculated. Then, the DTW correlation coefficients of the wavelet series after the six-level MODWT are computed as a comparison. The comparison results are shown in Table 5.

As seen from the table, we only obtain one value to represent the correlation degree between the bivariate series according to the Pearson and Kendall correlations, while we can gain a vector consisting of seven correlation coefficients based on the six-level MODWT and DTW. Taking the first set of bivariate time series in the table as an example, we cannot obtain the appropriate correlation coefficient by the Pearson or Kendall methods because of the influence of the sine function. However, we can obtain a more reasonable value from a higher level DTW correlation coefficient (for example, 0.9417) to indicate the correlation degree. We can also calculate the correlation degree of the time series from different resolutions and obtain quite different values. Therefore, we construct seven complex networks based on different resolutions (decomposition levels), and thus we can analyze the correlation patterns from multiple viewpoints rather than one.

**Result of wavelet decomposition:** The results of one smooth trend and the six-level wavelet details decomposed from PAB and BGH are illustrated in Fig. 3. As the decomposition level increases, the frequencies of fluctuations become lower, and the curves become smoother. Most of the volatilities in the PAB and BGH stock series are captured by the wavelet series on the high-resolution (i.e., D1–D2), the medium-resolution (i.e., D3–D4) and the low-resolution (i.e., D5–S6) scales.

The wavelet decomposition is equivalent to a feature extraction process. Different features can be extracted with the changing of the scale and location of the mother wavelet. Here, features refer to the fluctuation status obtained by observing the raw series on different resolutions. Thus, if the aim is to observe the dynamic fluctuations in a short time horizon, we should apply the high-resolution analysis. However, if the purpose is to mine the long-term trend, we should select the wavelet series with a higher decomposition level.

#### 4.3. Multi-resolution evolution of statistical features

In the process of defining second-level symbols, we set the threshold  $\omega$  of correlation lengths to determine the second-level symbol, which helps to observe the evolution of the correlation between time series from a more profound perspective. From Fig. 4, we notice the number of correlation lengths decreases as the correlation length increases. Furthermore, the number of correlation lengths is mostly concentrated in the range of 0–50, while only a few points are located in the domain of larger lengths. We select the optimal threshold according to the core idea of the classical OTSU algorithm [53] in image segmentation: the maximum variance between classes, and the minimum variance within a class. Based on the discriminant criterion, the optimal symbolic thresholds of six wavelet details and the smoothed trend are all 8. Moreover, the threshold point is exactly the inflection point of the fitting curve (see the vertical red line in Fig. 4).

Theoretically, based on the coarse-graining process, we should obtain 46 656 ( $6^6 =$ ) types of correlation patterns for each time scale. However, the number of correlation patterns varies with the different levels of the MODWT and ranges from 366 to 23, which is far less than 46656. Fig. 5 illustrated the number of the correlation patterns and the number of edges at different levels of MODWT. On the high-resolution scale (D1–D2) and the medium-resolution scale (D3–D4), the number of patterns and edges is much higher than that of the low-resolution scale (D5–S6). From the medium-resolution scale to the low-resolution scale, there is a sharp decrease in the number of patterns and edges. In addition, the smooth trend S6 has the least number of patterns and edges. This behavior implies that the correlation features between the PAB and BGH closing prices become more unitary as the scale enlarges. Furthermore, on the medium-resolution scale, there is a transition process from a weak or uncorrelated pattern on the high-resolution scale to a strong correlation on the low-resolution scale, and the number of correlation patterns on the medium-resolution scale is relatively stable.

#### 4.4. Key correlation patterns in the transition process

The weighted degree is a comprehensive indicator of the importance of a node [7]. This measure considers not only the number of a node's neighbors, but also the weight of the connection between a node and an adjacent node. Hence, in the transition process, the weighted degree is more suitable than other measures to indicate the importance of correlation patterns. The definition of weighted degree is calculated as follows:

$$w_i = w_i^{in} + w_i^{out} = \sum_{j \in N_i} w_{ji} + \sum_{j \in N_i} w_{ij} \quad (9)$$

where  $N_i$  denotes the set of the nodes connecting to node  $i$ ,  $w_{ij}$  denotes the weight of the edge from node  $i$  to node  $j$ , and  $w_{ji}$  denotes the weight of the edge from node  $j$  to node  $i$ .

After ranking the nodes by the weighted degree, we can identify four key correlation patterns at each decomposition level (Fig. 6). On the low-resolution scale, the number of weighted degrees is much smaller than that on the high-resolution and middle-resolution scales, while the percentage of the total weighted degree of the low-resolution scale increases rapidly after the middle-resolution scale because the number of nodes on the low-resolution scale is less than another period (Fig. 5). Moreover, the key correlation patterns tend to convert to those patterns that also have a higher weighted degree, and some key correlation patterns sometimes convert to each other (see the unidirectional and double arrow in Fig. 6). In other words, the key correlation patterns can control the randomness of the transition process.

#### 4.5. Discovering the critical modes between the bull market and bear market on the high-resolution scale

When a stock market is in the state of a bull market, we should be

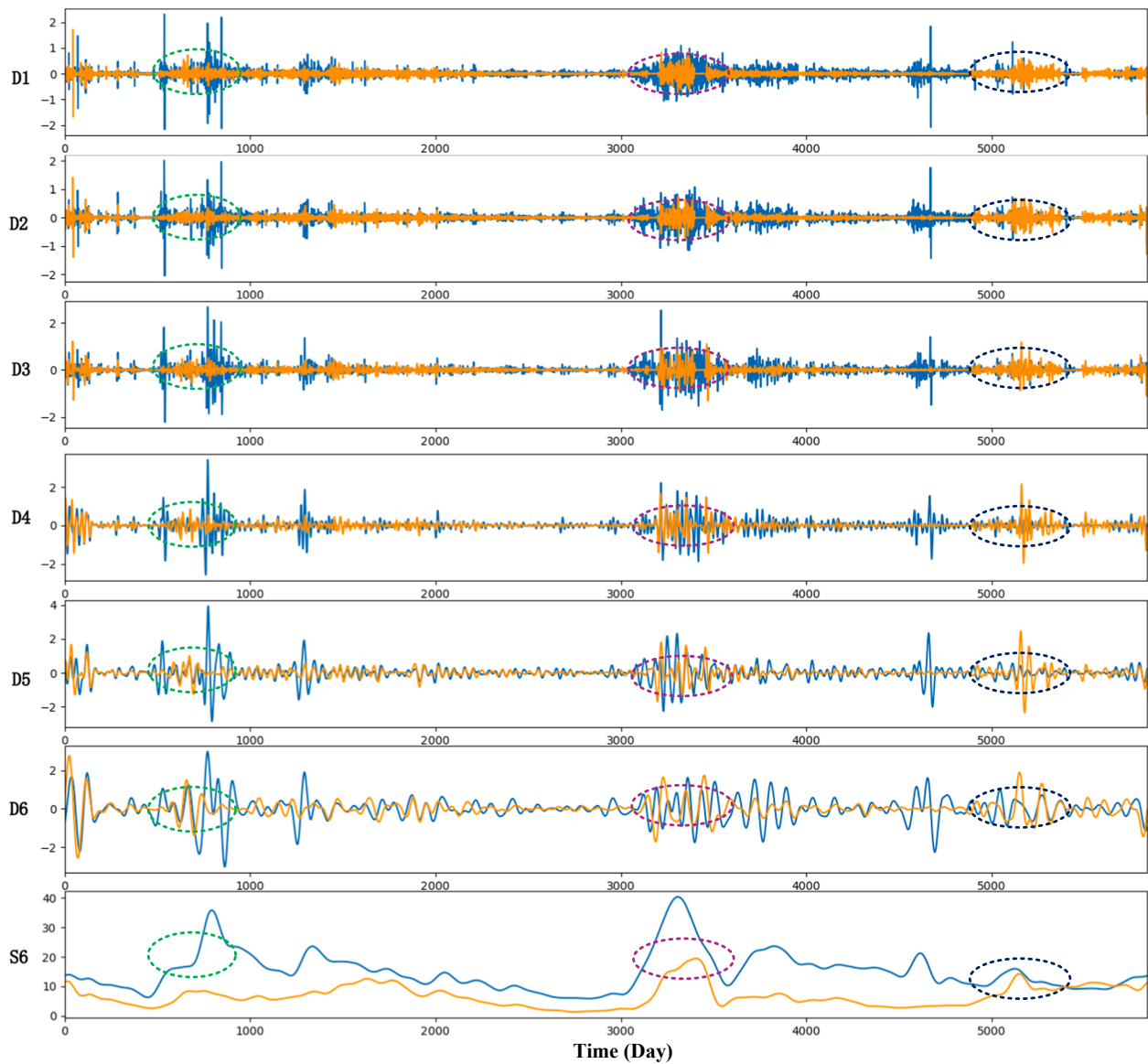


**Fig. 3.** MODWT decomposition results for PAB and BGH closing prices.

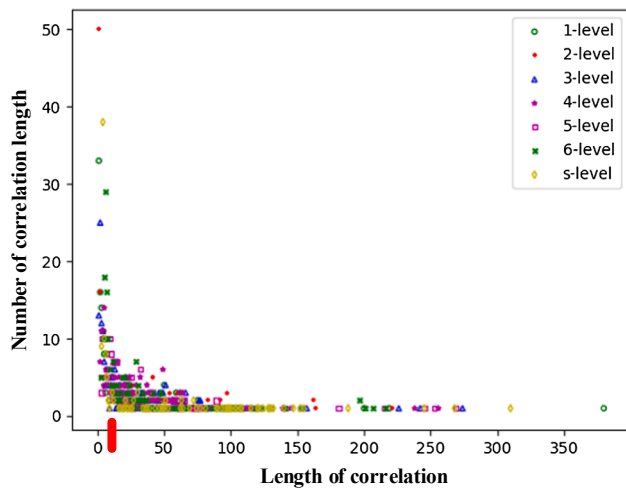


**Fig. 4.** The procedure of selecting optimal thresholds on different scales.

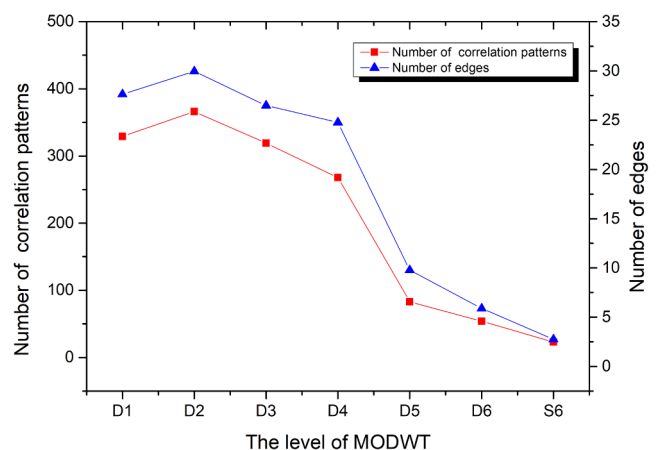


**Fig. 5.** Variation of the number of the correlation patterns and edges at different levels of MODWT.

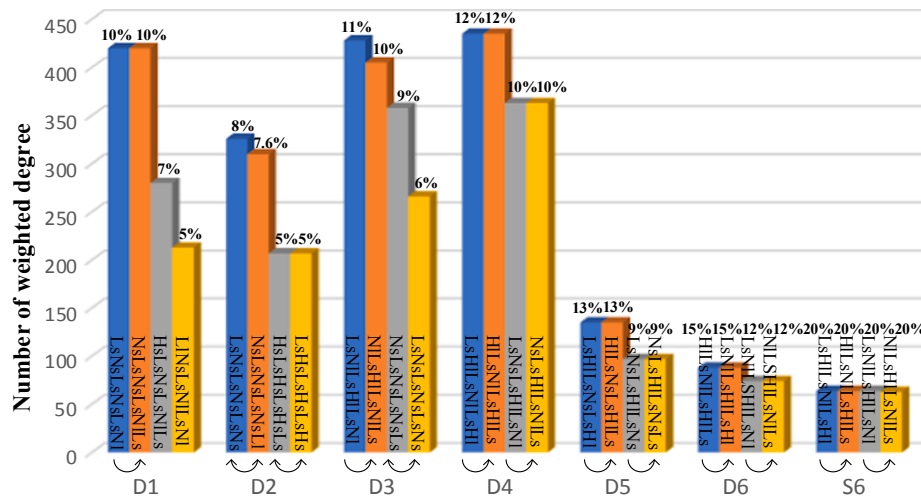


Fig. 6. Top four dominant correlation modes on different scales.

aware of the arrival of the bear market. Conversely, we desire to seize the opportunity to turn to the bull market when in a bear state. Therefore, it is meaningful to reveal the critical modes between the bull market and the bear market. The critical value is a more precise amount, so we should analyze it from a micro-perspective rather than a macro-perspective. Therefore, experiments revealing the critical modes are performed based on the high-resolution scale (D1-D2). The transmission intermediary is a topological characteristic of complex networks. When the intermediary modes appear, it indicates that the moment is in a transitional period. The level of the transmission intermediary shows the capability of controlling information during the transmission process. Other modes can only transmit to others through the intermediary modes. The centrality describes the position of a node in the network, which denotes the ability of the node as an intermediary. Therefore, it is feasible to find intermediary modes by employing betweenness centrality. Moreover, the critical modes are exactly the intermediary modes between the bull market and the bear market because the modes in the bull market and bear market can only transmit to others through the critical modes. Hence, we perform data analysis to prove that the intermediary modes can be seen as the potential critical modes. First, we calculate the normalizing betweenness centrality  $BC_i$  of node  $i$ , and the definition is as follows [54,55]:

$$BC_i = \frac{\sum_j^n \sum_k^n q_{jk}(i)/q_{jk}}{n^2 - 3n + 2}, \quad j \neq k \neq i, \quad j < k \quad (10)$$

where  $q_{jk}$  is the total number of shortest paths between nodes  $j$  and  $k$ .  $q_{jk}(i)$  is the number of shortest paths between nodes  $j$  and  $k$  that pass the node  $i$ .

A higher value of betweenness centralities means a stronger transmission ability of correlation modes. The evolution of betweenness centrality on the scale D1 and D2 is displayed in Fig. 7. According to the value of betweenness centralities, we pick the first three patterns as the intermediary patterns. Then, we find the corresponding time periods of these six intermediary patterns in the original time series. For example, mapping to the time domain, the mode  $NsLsNsLsNlS$  is a sub-series of the original time series ranging from 1996.09.18 to 1996.12.09 and 2007.11.07 to 2008.01.04. The time points contained in each pattern may be of great quantity due to the two-level symbolization. Therefore, we can use the top-down approach to identify bull and bear markets, which was proposed by Alan J. Hanna in 2017 [56]. Based on this detection method, we test whether there is a bullish or bearish state in the sub-series corresponding to intermediary modes. Although there are three fault detection results (Fig. 8), we can conclude that the intermediary modes obtained by betweenness centrality are exactly the critical patterns because most of the conversion phases are correctly

detected. Because of the two-level symbolization in the process of building complex networks, we discarded some local information in exchange for the trajectory of fluctuations. Meanwhile, the specific label is determined by the threshold, and the division of the correlation level near the threshold is blurred. The calculation of betweenness centrality is based on correlation patterns, so error detection may occur due to the existence of minor deviations in the coarse-graining process. In addition, there are two kinds of fault detection results. One is the single-error detection that occurs when one time series has a transition between bull and bear states and another time series does not. The other one is the absolute-error detection that occurs when there is no critical period in both series, but it is detected by the intermediary modes. In Fig. 8, the middle error detection indicated by the grey transparent bar is an absolute-error detection while the other two error detections are single-error detections. Observing the critical patterns above, we also find that the symbols  $Nl$  and  $Ns$  account for a high proportion. In other words, during the transition between the bull market and the bear market, the stock markets are of less relevance due to the abnormal stock fluctuations.

#### 4.6. Clustering effect analysis of the financial crisis on the middle-resolution scale

Based on the key correlation patterns, we find that some correlation patterns convert to each other more frequently rather than other correlation patterns. This phenomenon makes some correlation patterns and their relations form some clusters. The correlation patterns in a cluster connect relatively closely to each other, so each cluster represents a special transition type.

According to Fig. 3, all the time series have changed dramatically from July 1997 to June 1998, from August 2007 to December 2008 and from July 2015 to September 2016 (see the dotted circle with different colors). Meanwhile, the dramatic changes coincide with the Asian financial crisis that began in 1997, the global financial crisis that occurred in 2008, and the Chinese stock markets disaster in 2015. These dramatic changes in the stock markets have also been proven by previous studies [57–59]. We investigate the cluster distribution during the financial crisis periods to explore the transition type of correlation patterns. The duration of a financial crisis is generally more than one year, so the high resolution is not suitable for analysis because excessive details may cover the special features of the crisis stage. Hence, we choose the middle resolution (D3-D5) for analysis because there are too few nodes in the low-resolution network to reveal the disciplines of the financial crisis. First, we find the corresponding patterns during the three financial crisis stages; then, the correlation patterns are marked as

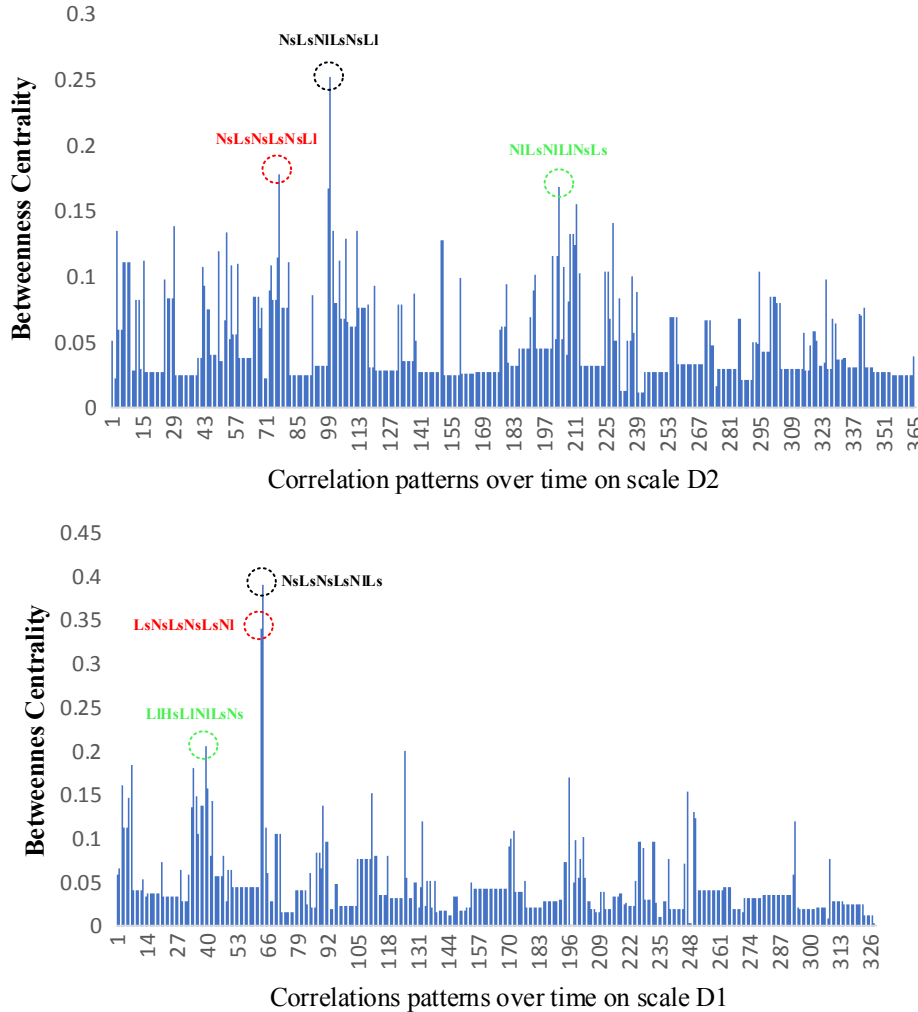


**Fig. 7.** The evolution of betweenness centrality on the scale D1 and D2. We pick the specific correlation modes with higher betweenness centralities on each scale, e.g.,  $NsLsNsLsNsNL$  (0.39),  $LsNsLsNsLsNL$  (0.34) and  $LIHsLINILsNs$  (0.20) on scale D1.

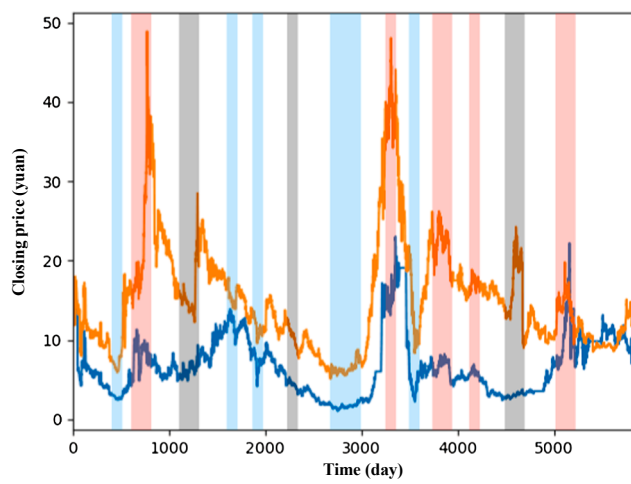


**Fig. 8.** The results of critical modes detection. The blue transparent bars indicate there are turning periods from bear states to bull states, the pink transparent bars indicate there are turning periods from bull states to bear states, the grey transparent bars denote there is no critical period but detected by the intermediary modes. (For interpretation of the references to color in this figure legend, the reader is referred to the web version of this article.)

crisis0, crisis1 and crisis2 to denote the stock markets disaster, global economic crisis and Asian financial crisis. According to Fig. 9, the networks of scale D3 and D4 are all divided into six clusters. In addition, we can see that both crisis0 and crisis1 are limited to a single cluster, in addition to few transition modes in the dotted circles. The global financial crisis belongs to the subprime crisis while the stock disaster in 2015 is a substance crisis with different crisis features. Compared with the crisis in 2008, the crisis in 2015 represents purely technical funding-driven fluctuations, and China's economic fundamentals have not deteriorated significantly. Additionally, the duration of abnormal fluctuations is less than the former. Therefore, the modes of the global financial crisis and stock disaster are in different clusters due to the different crisis features [60,61]. Moreover, the Asian financial crisis is also a subprime crisis, so it shares some features with the global crisis. In addition, China's economy has not been significantly affected because of the implementation of the RMB protection policy, which is roughly similar to the stock market disaster. Sharing the crisis features with the global crisis and stock disaster, the modes of the Asian crisis exist in the two clusters. Furthermore, the percentages of label H1 and label Hs increase rapidly during the three crises. The reason is that almost all the stocks fell during the crisis, and the correlation degree is enhanced. The clustering effect of the financial crisis on scale D5 is similar; however, it is not shown in this paper given the article structure.

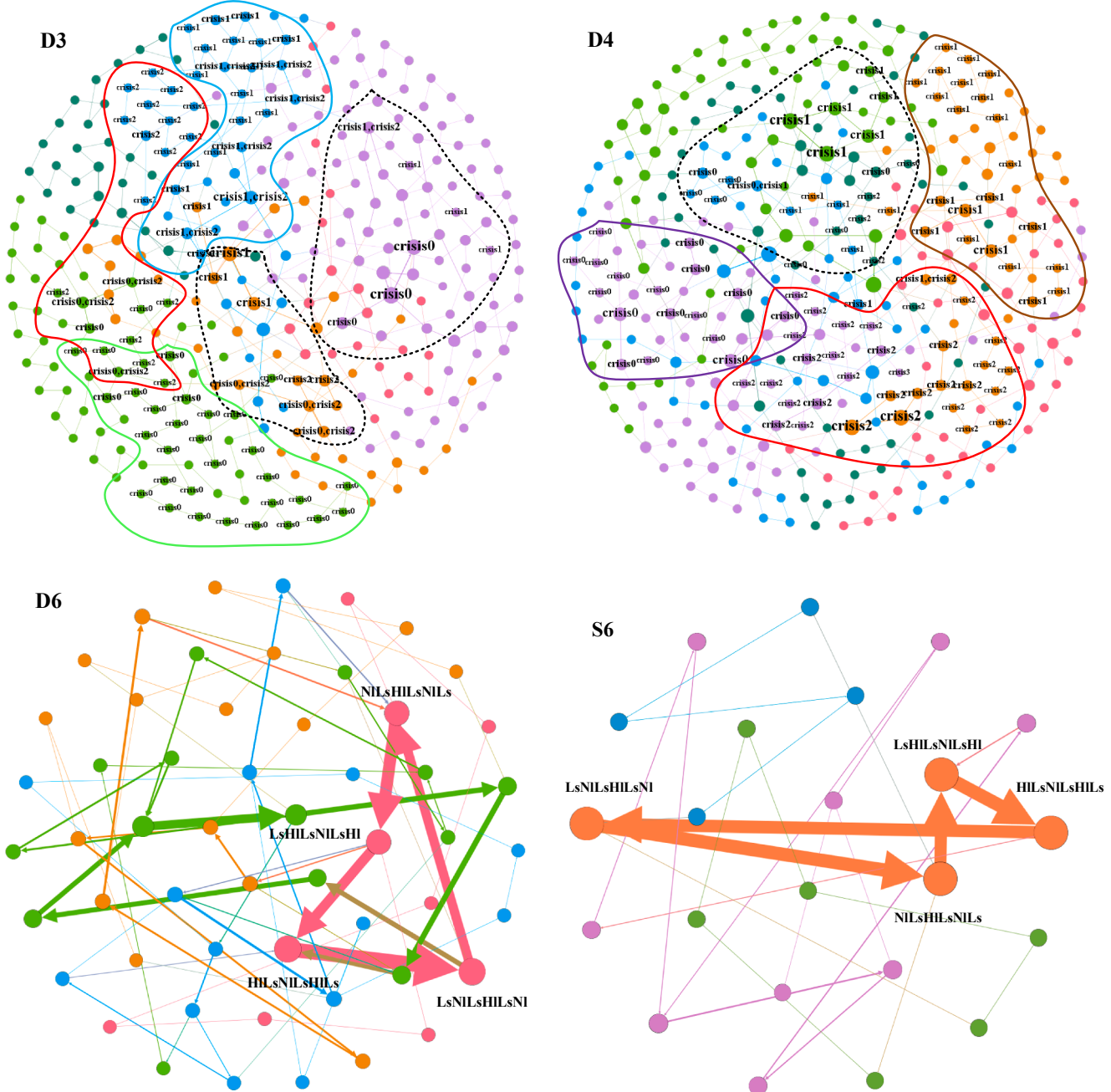


**Fig. 9.** The clustering effect of correlation modes on different decomposition scales. The modes on different crises are circled by a solid curve with a different color, while the virtual curve circles the modes that are the transition modes between the crisis stage and the normal stage on D3 and D4.

#### 4.7. Detection of potential pseudo cycles on the low-resolution scale

To guide the investors from the macro-perspective, we discuss the correlation modes on the low-resolution scale (D6-S6). We discover that there is a mode cycle with the highest weighted degree in both networks on scale D6 and S6, respectively (Fig. 9). Cycles on scale D6 and S6 are both  $HILsNILsHILs-LsNILsHILsNl-NILsHILsNILs-LsHILsNILsHILs-HILsNILsHILs$ . Moreover, these four modes form a cluster independently, and they transform to each other with high probability. Therefore, the mode cycle can be seen as the potential pseudo cycle of the stock market. Due to the uncertainty of the correlation length, the duration of these cycles is not exactly the same. However, by knowing the approximate transition trajectory of correlation modes, investors can also predict the next possible correlation pattern to make more reasonable decisions.

#### 5. Conclusions

The correlation between the closing prices of PAB and BGH has different fluctuation features in different time-frequency domains. In this paper, to study the transmission characteristics of the time-varying relations between bivariate time series from a multi-resolution perspective, we have proposed a hybrid approach combining wavelet analysis and complex network theory.

After designing the multi-resolution evolutionary complex networks, we examine the statistical characteristics to provide investors with more information that cannot be captured by conventional analysis. By investigating the correlation modes in the dominating position, we know that the key correlation modes tend to convert to those modes that also have a higher weighted degree, while some key correlation patterns sometimes convert to each other. Thus, the state of the market

is guided by these key correlation patterns. Recognizing the key modes can provide useful information to make more dynamic and well-adapted decisions.

Finally, we analyze the typical features of the stock market from different resolutions to guide investors or policy makers to make sensible decisions and avoid risks. On the high-resolution scale, we verify the feasibility of regarding intermediary modes as the potential critical modes between the bull market and the bear market. The global financial crisis and stock disaster have different crisis features, while the Asian financial crisis in 1997 exhibits shared features with them, according to the clustering effect on the middle-resolution scale. Furthermore, the potential cycles of the stock market have been found by integrating the dominant nodes and cluster effect on the low-resolution scale. By analyzing different states in the stock market from different resolutions, we find that the results of these experiments exactly match reality, providing powerful evidence to prove that our method is effective in financial time series analysis. However, due to the two-level symbolization in the process of building complex networks, we discard some local information in exchange for the trajectory of fluctuations, and the number of nodes decreases sharply. Meanwhile, the specific label is determined by the threshold, so the division of the correlation level near the threshold is blurred.

Moreover, we only consider the closing price of the two stocks, while other factors, such as transaction price, turnover rate, etc., are not considered. Therefore, in the future, we will conduct some further research to reveal the underlying law of the stock market. On one hand, we will explore the evolutionary characteristics of correlation patterns among multivariate time series; on the other hand, we will consider multiple factors affecting the stocks through information fusion. Ultimately, the goal of our further study is to provide investors with more reasonable investment portfolios.

## Declaration of Competing Interest

There are no conflicts of interest

## Acknowledgements

This work is supported by the National Key R&D Program of China, Grant No. is 2016YFC1401900.

## References

- [1] R. Efendia, N. Arbayi, M.M. Deris, A new procedure in stock market forecasting based on fuzzy random auto-regression time series model, *Inf. Sci. (Ny)*. 441 (2018).
- [2] M. Wang, A.L.M. Vilela, L. Tian, H. Xu, R. Du, A new time series prediction method based on complex network theory, in: Proc. - 2017 IEEE Int. Conf. Big Data, Big Data 2017, 2018-Jan (2018) pp. 4170–4175. doi: <https://doi.org/10.1109/BigData.2017.8258440>.
- [3] S. Huang, H. An, X. Gao, X. Hao, X. Huang, The multiscale conformation evolution of the financial time series, *Math. Probl. Eng.* 2015 (2015) 1–9, <https://doi.org/10.1155/2015/563145>.
- [4] C. Feng, B. He, Construction of complex networks from time series based on the cross correlation interval, *Open Phys.* 15 (2017) 253–260, <https://doi.org/10.1515phys-2017-0028>.
- [5] X. Gao, H. An, W. Fang, X. Huang, H. Li, W. Zhong, Characteristics of the transmission of autoregressive sub-patterns in financial time series, *Sci. Rep.* 4 (2014) 1–9, <https://doi.org/10.1038/srep06290>.
- [6] X. Gao, H. An, W. Fang, H. Li, X. Sun, The transmission of fluctuant patterns of the forex burden based on international crude oil prices, *Energy* 73 (2014) 380–386, <https://doi.org/10.1016/j.energy.2014.06.028>.
- [7] M. Jiang, X. Gao, H. An, H. Li, B. Sun, Reconstructing complex network for characterizing the time-varying causality evolution behavior of multivariate time series, *Sci. Rep.* 7 (2017) 1–12, <https://doi.org/10.1038/s41598-017-10759-3>.
- [8] Z. Gao, S. Li, Q. Cai, W. Dang, Y. Yang, C. Mu, P. Hui, Relative wavelet entropy complex network for improving EEG-based fatigue driving classification, *IEEE Trans. Instrum. Meas.* (2018) 1–8, <https://doi.org/10.1109/TIM.2018.2865842>.
- [9] Z. Gao, W. Dang, C. Mu, Y. Yang, S. Li, C. Grebogi, A novel multiplex network-based sensor information fusion model and its application to industrial multiphase flow system, *IEEE Trans. Ind. Inform.* 14 (2018) 3982–3988, <https://doi.org/10.1109/TII.2017.2785384>.
- [10] X. Huang, H. An, X. Gao, X. Hao, P. Liu, Multiresolution transmission of the correlation modes between bivariate time series based on complex network theory, *Phys. A Stat. Mech. Appl.* 428 (2015) 493–506, <https://doi.org/10.1016/j.physa.2015.02.028>.
- [11] Z.-K. Gao, S. Li, W.-D. Dang, Y.-X. Yang, Y. Do, C. Grebogi, Wavelet multiresolution complex network for analyzing multivariate nonlinear time series, *Int. J. Bifurc. Chaos*. (2017), <https://doi.org/10.1142/s0218127417501231>.
- [12] Z. Gao, K. Zhang, W. Dang, Y. Yang, Z. Wang, H. Duan, G. Chen, An adaptive optimal-Kernel time-frequency representation-based complex network method for characterizing fatigued behavior using the SSVEP-based BCI system, *Knowledge-Based Syst.* 152 (2018) 163–171, <https://doi.org/10.1016/j.knosys.2018.04.013>.
- [13] S.G. Mallat, A theory for multiresolution signal decomposition: the wavelet representation, *IEEE Trans. Pattern Anal. Mach. Intell.* 11 (1989) 674–693, <https://doi.org/10.1109/34.192463>.
- [14] M. Wang, L. Tian, From time series to complex networks: The phase space coarse graining, *Phys. A Stat. Mech. Appl.* 461 (2016) 456–468.
- [15] J. Zhang, J. Sun, X. Luo, K. Zhang, NAKAMURA, Tomomichi, Michael, Characterizing pseudoperiodic time series through the complex network approach, *Phys. D Nonlinear Phenom.* 237 (2008) 2856–2865.
- [16] Z.K. Gao, M. Small, J. Kurths, Complex network analysis of time series, *EPL (Europhys. Lett.)* 116 (2016) 50001.
- [17] L. Fei, Q. Zhang, Y. Deng, Identifying influential nodes in complex networks based on the inverse-square law, *Phys. A Stat. Mech. Appl.* 512 (2018) 1044–1059, <https://doi.org/10.1016/J.PHYSA.2018.08.135>.
- [18] R. Zhang, B. Ashuri, Y. Deng, A novel method for forecasting time series based on fuzzy logic and visibility graph, *Adv. Data Anal. Classif.* 11 (2017) 759–783, <https://doi.org/10.1007/s11634-017-0300-3>.
- [19] M.G. Carneiro, L. Zhao, Organizational data classification based on the importance concept of complex networks, *IEEE Trans. Neural Netw. Learn Syst.* (2017) 1–13.
- [20] S. Supriya, S. Siuly, H. Wang, Y. Zhang, EEG Sleep stages analysis and classification based on weighed complex network features, 2018, doi: <https://doi.org/10.1109/TETC.2018.2876529>.
- [21] N. Yuan, Z. Fu, H. Zhang, L. Piao, E. Xoplaki, J. Luterbacher, Detrended partial-cross-correlation analysis: a new method for analyzing correlations in complex, *System* (2015), <https://doi.org/10.1038/srep08143>.
- [22] K. Shi, J. Wang, S. Zhong, X. Zhang, Y. Liu, J. Cheng, New reliable nonuniform sampling control for uncertain chaotic neural networks under Markov switching topologies, *Appl. Math. Comput.* 347 (2019) 169–193, <https://doi.org/10.1016/J.AMC.2018.11.011>.
- [23] P. Xu, R. Zhang, Y. Deng, A novel visibility graph transformation of time series into weighted networks, *Chaos, Solitons Fractals* 117 (2018) 201–208, <https://doi.org/10.1016/J.CHAOS.2018.07.039>.
- [24] K. Shi, Y. Tang, S. Zhong, C. Yin, X. Huang, W. Wang, Nonfragile asynchronous control for uncertain chaotic Lurie network systems with Bernoulli stochastic process, *Int. J. Robust Nonlinear Control* 28 (2018) 1693–1714, <https://doi.org/10.1002/rnc.3980>.
- [25] J. Wang, K. Shi, Q. Huang, S. Zhong, D. Zhang, Stochastic switched sampled-data control for synchronization of delayed chaotic neural networks with packet dropout, *Appl. Math. Comput.* 335 (2018) 211–230, <https://doi.org/10.1016/j.amc.2018.04.038>.
- [26] L. Lacasa, B. Luque, F. Ballesteros, J. Luque, J.C. Nuno, From time series to complex networks: the visibility graph, (2008) pp. 1–13. doi: <https://doi.org/10.1073/pnas.0709247105>.
- [27] A. Szolnoki, Z. Wang, M. Perc, Wisdom of groups promotes cooperation in evolutionary social dilemmas, 2012. doi: <https://doi.org/10.1038/srep00576>.
- [28] Z. Wang, A. Szolnoki, M. Perc, Optimal interdependence between networks for the evolution of cooperation, 2013, doi: <https://doi.org/10.1038/srep02470>.
- [29] X. Sun, H. An, X. Gao, X. Jia, X. Liu, Indirect energy flow between industrial sectors in China: A complex network approach, 2016. doi: <https://doi.org/10.1016/j.energy.2015.10.102>.
- [30] X. Gao, H. An, W. Fang, X. Huang, H. Li, W. Zhong, Characteristics of the transmission of autoregressive sub-patterns in financial time series, *Sci. Rep.* 4 (2014) 6290.
- [31] R. Wackerbauer, A. Witt, H. Atmanspacher, J. Kurths, H. Scheingraber, A comparative classification of complexity measures, 1994. doi: [https://doi.org/10.1016/0960-0779\(94\)90023-X](https://doi.org/10.1016/0960-0779(94)90023-X).
- [32] C. Liu, W.-X. Zhou, W.-K. Yuan, Statistical properties of visibility graph of energy dissipation rates in three-dimensional fully developed turbulence, 2010. doi: <https://doi.org/10.1016/j.physa.2010.02.043>.
- [33] J. Tang, Y. Wang, H. Wang, S. Zhang, F. Liu, Dynamic analysis of traffic time series at different temporal scales: A complex networks approach, *Phys. A Stat. Mech. Appl.* 405 (2014) 303–315.
- [34] J.F. Donges, R.V. Donner, M.H. Trauth, M. Norbert, S. Hans-Joachim, K. Jürgen, Nonlinear detection of paleoclimate-variability transitions possibly related to human evolution, *Proc. Natl. Acad. Sci. U. S. A.* 108 (2011) 20422–20427.
- [35] J. Zhang, W. Cheng, Z. Liu, K. Zhang, X. Lei, Y. Yao, B. Becker, Y. Liu, K.M. Kendrick, G. Lu, Neural, electrophysiological and anatomical basis of brain-network variability and its characteristic changes in mental disorders, *Brain* 139 (2016) 2307–2321.
- [36] Z.-K. Gao, P.-C. Fang, M.-S. Ding, N.-D. Jin, Multivariate weighted complex network analysis for characterizing nonlinear dynamic behavior in two-phase flow, 2015. doi: <https://doi.org/10.1016/j.jepthermflusci.2014.09.008>.
- [37] H. Yang, Y. Deng, J. Jones, Network Division Method Based on Cellular Growth and Physarum-inspired Network Adaptation, *Int. J. Unconv. Comput.* 13 (2018) 477–491.
- [38] J. Zhang, M. Small, Complex network from pseudoperiodic time series: topology

- versus dynamics, *Phys. Rev. Lett.* 96 (2006) 238701.
- [39] N. Marwan, J.F. Donges, Y. Zou, R.V. Donner, J. Kurths, Complex network approach for recurrence analysis of time series, *Phys. Lett. A* 373 (2009) 4246–4254.
- [40] X. Gao, W. Fang, F. An, Y. Wang, Detecting method for crude oil price fluctuation mechanism under different periodic time series, *Appl. Energy* 192 (2017) 201–212, <https://doi.org/10.1016/j.apenergy.2017.02.014>.
- [41] K. He, K.K. Lai, J. Yen, Ensemble forecasting of Value at Risk via Multi Resolution Analysis based methodology in metals markets, *Expert Syst. Appl.* 39 (2012) 4258–4267.
- [42] L.J. Kao, C.C. Chiu, C.J. Lu, C.H. Chang, A hybrid approach by integrating wavelet-based feature extraction with MARS and SVR for stock index forecasting, *Decis. Support Syst.* 54 (2013) 1228–1244.
- [43] S. Huang, H. An, H. Xuan, X. Jia, Co-movement of coherence between oil prices and the stock market from the joint time-frequency perspective, *Appl. Energy* 221 (2018) 122–130.
- [44] S. Dajčman, Interdependence between some major European stock markets - a wavelet lead/lag analysis, *Prague Econ. Pap.* 2013 (2013) 28–49.
- [45] R. Gençay, F. Selçuk, B. Whitcher, Differentiating intraday seasonalities through wavelet multi-scaling, *Phys. A Stat. Mech. Appl.* 289 (2001) 543–556.
- [46] M.R. Chernick, *Wavelet Methods for Time Series Analysis*, 2004.
- [47] M.J. Shensa, The discrete wavelet transform: wedding the a trous and Mallat algorithms, *IEEE Trans. Signal Process.* 40 (1992) 2464–2482.
- [48] H. Sakoe, S. Chiba, Dynamic programming algorithm optimization for spoken word recognition, *IEEE Trans. Acoust. Speech Signal Process.* 26 (2003) 43–49.
- [49] R. Meszlenyi, P. Hermann, K. Buza, V. Gál, Z. Vidnyánszky, Resting state fMRI functional connectivity analysis using dynamic time warping, 2017. doi: <https://doi.org/10.3389/fnins.2017.00075>.
- [50] G.S. Uddin, S. Bekiros, A. Ahmed, The nexus between geopolitical uncertainty and crude oil markets: An entropy-based wavelet analysis  $\star$ , *Phys. A Stat. Mech. Appl.* 495 (2018) 30–39.
- [51] S. Bekiros, M. Marcellino, The multiscale causal dynamics of foreign exchange markets  $\star$ , *J. Int. Money Financ.* 33 (2013) 282–305.
- [52] J. Chae, D. Thom, H. Bosch, J. Yun, R. Maciejewski, D.S. Ebert, T. Ertl, Spatiotemporal social media analytics for abnormal event detection and examination using seasonal-trend decomposition, in: T.B.T.-I.C. on V.A.S.& T., 2012.
- [53] N. Ohtsu, A threshold selection method from gray-level histograms, *IEEE Trans. Syst. Man Cybern.* 9 (2007) 62–66.
- [54] X. Gao, H. An, F. Wei, H. Li, X. Sun, The transmission of fluctuant patterns of the forex burden based on international crude oil prices, *Energy* 73 (2014) 380–386.
- [55] L.C. Freeman, Centrality in social networks conceptual clarification, *Soc. Networks* 1 (1978) 215–239.
- [56] A.J. Hanna, A top-down approach to identifying bull and bear market states, *Int. Rev. Financ. Anal.* 55 (2017) 93–110.
- [57] D. Sornette, G. Demos, Q. Zhang, P. Cauwels, Q. Zhang, Real-time prediction and post-mortem analysis of the Shanghai 2015 stock market bubble and crash, *Soc. Sci. Electron. Publ.* (2015).
- [58] M.L. Lemmon, K.V. Lins, Ownership structure, corporate governance, and firm value: evidence from the East Asian financial crisis, *J. Finance* 58 (2003) 1445–1468.
- [59] J. Crotty, Structural causes of the global financial crisis: a critical assessment of the “new financial architecture”, *Cambridge J. Econ.* 33 (2009) 563–580.
- [60] Y. Rui, X. Li, Z. Tong, Analysis of linkage effects among industry sectors in China's stock market before and after the financial crisis, *Phys. A Stat. Mech. Appl.* 411 (2014) 12–20.
- [61] W.H. Hu, G. Fei, C. Chao, Financial crisis prediction based on distance to default and feature weighted support vector machine, in: H.B.T.-I.C. on N., 2016.